

# HiRED: Attention-Guided Token Dropping for Efficient Inference of High-Resolution Vision-Language Models in Resource-Constrained Environments

Kazi Hasan Ibn Arif<sup>1</sup>, JinYi Yoon<sup>1</sup>, Dimitrios S. Nikolopoulos<sup>1</sup>, Hans Vandierendonck<sup>2</sup>, Deepu John<sup>3</sup>, Bo Ji<sup>1</sup>

<sup>1</sup>Virginia Tech, Blacksburg, VA, USA

<sup>2</sup>Queen's University Belfast, Belfast, UK

<sup>3</sup>University College Dublin, Dublin, Ireland

## Abstract

High-resolution Vision-Language Models (VLMs) have been widely used in multimodal tasks to enhance accuracy by preserving detailed image information. However, these models often generate excessive visual tokens due to encoding multiple partitions of the input image. Processing these excessive visual tokens is computationally challenging, especially in resource-constrained environments with commodity GPUs. To support high-resolution images while meeting resource constraints, we propose *High-Resolution Early Dropping (HiRED)*, a token-dropping scheme that operates within a fixed token budget before the Large Language Model (LLM) stage. HiRED can be integrated with existing high-resolution VLMs in a plug-and-play manner, as it requires no additional training while still maintaining superior accuracy. We strategically use the vision encoder's attention in the initial layers to assess the visual content of each image partition and allocate the token budget accordingly. Then, using the attention in the final layer, we select the most important visual tokens from each partition within the allocated budget, dropping the rest. Empirically, when applied to LLaVA-Next-7B on NVIDIA TESLA P40 GPU, HiRED with a 20% token budget increases token generation throughput by  $4.7\times$ , reduces first-token generation latency by 15 seconds, and saves 2.3 GB of GPU memory for a single inference. The code is available at <https://github.com/hasanar1f/HiRED>.

## 1 Introduction

Vision-Language Models (VLMs), such as GPT-4v (Achiam et al. 2023), Gemini Pro (Reid et al. 2024), LLaVA (Li et al. 2023a), and Qwen-VL (Bai et al. 2023), have emerged as remarkable multimodal models that learn from visual and textual data. However, these VLMs inherently rely on low-resolution image encodings, which makes it challenging to process high-resolution images, thus resulting in loss of fine-grained visual information (Zhang et al. 2024a; Dong et al. 2024). To address this issue, recent VLMs, referred to as high-resolution VLMs, employ *dynamic partitioning* to encode high-resolution images (Liu et al. 2024a; Dong et al. 2024; Li et al. 2024b; Liu et al. 2024b; Lin et al. 2023; Chen, Pekis, and Brown 2024).

A typical inference pipeline of high-resolution VLMs with dynamic partitioning is illustrated in Fig. 1. Specifically, a high-resolution input image is partitioned into multiple low-resolution sub-images (e.g., four sub-images for a

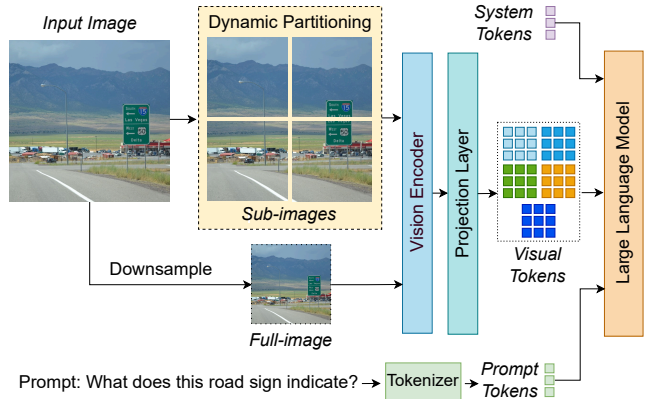


Figure 1: Inference steps of LLaVA-Next (Liu et al. 2024a) for a high-resolution VLM with dynamic partitioning.

square image in LLaVA-Next); a downsampled version of the original image, referred to as the full-image, is also included. Subsequently, a vision encoder such as Vision Transformers (ViTs) encodes each low-resolution image partition into image features, which are then converted to visual tokens in the text embedding space by a lightweight Projection Layer. These visual tokens are concatenated together and fed into a Large Language Model (LLM) (along with prompt tokens and system tokens) for generating the final response.

Here, the image partitions have different spatial distributions of image contents and possess various levels of information, thus exhibiting different degrees of importance. While the full-image captures the global context of the original image, each sub-image is for a more detailed local representation of corresponding specific areas. This multi-partitioning approach enables the inclusion of more visual details, which can significantly boost the model accuracy. For example, MM1 (McKinzie et al. 2024) can improve accuracy by 15% when increasing the image resolution from  $336\times 336$  to  $1344\times 1344$ .

However, due to the need to encode multiple image partitions, high-resolution VLMs often generate 3-10 times more visual tokens than low-resolution VLMs (Dong et al. 2024; Hu et al. 2024). Such excessive visual tokens result in lower inference throughput, increased generation latency, and higher GPU memory usage. Furthermore, depending

Table 1: Comparison between our HiRED and existing methods.

Method	High Resolution	Resource Constraint	Early Dropping	Task Coverage
FastV (Chen et al. 2024)	✗	✓	✗	✓
FlexAttention (Li et al. 2024a)	✓	✗	✗	✓
TokenCorrCompressor (Zhang et al. 2024c)	✓	✗	✓	✗
PruMerge (Shang et al. 2024)	✗	✗	✓	✓
HiRED (Ours)	✓	✓	✓	✓

on downstream tasks, the number of visual tokens required to represent an image also varies significantly (Cai et al. 2024). However, most commodity GPUs, such as the Jetson Orin NX (8 or 16 GB) and NVIDIA Tesla T4 (16 GB), have limited computational cores and memory. The quadratic complexity of transformers makes it challenging to process a large number of tokens on these GPUs. In addition, increased key-value (KV) cache size due to storing token embeddings at runtime could cause out-of-memory issues. Therefore, controlling and optimizing the number of visual tokens is essential to meet the system resource constraints. Although traditional optimization techniques (e.g., model quantization, weight pruning, and lightweight architectures) can reduce model size, they do not address the critical issue of excessive visual tokens.

Therefore, we aim to achieve efficient inference of high-resolution VLMs under resource-constrained settings through strategic dropping of excessive visual tokens. Such token-dropping schemes are expected to offer four desired properties: (i) *Supporting high-resolution*: plug-and-play integration (i.e., without model training and architectural changes) that promotes easy adoption with existing high-resolution VLMs while maintaining superior accuracy; (ii) *Satisfying resource constraint*: having control over the number of visual tokens fed into the LLM decoding phase to enable efficient inference under various resource constraints and task requirements; (iii) *Facilitating early dropping*: dropping tokens in the image encoding stage (i.e., before the LLM decoding phase) to reduce input sequence length and enhance computational efficiency; and (iv) *Wide task coverage*: covering a wide range of vision-language tasks (visual question answering, image captioning, document understanding, etc.).

The recent few months have witnessed exciting progress towards the above goals (Chen et al. 2024; Li et al. 2024a; Zhang et al. 2024c; Shang et al. 2024). However, none of these works achieve all the aforementioned properties, which are highly desired for efficient high-resolution VLM inference in resource-constrained environments (see Table 1 for a summary and Section 2 for a detailed discussion).

**Contributions.** Our work bridges this critical gap and makes the following main contributions:

We propose *High-Resolution Early Dropping (HiRED)*, a plug-and-play token-dropping framework for efficient inference of high-resolution VLMs. HiRED enables attention-guided early dropping of visual tokens under resource constraints and covers a wide range of multimodal tasks. *To the*

*best of our knowledge, HiRED is the first framework that achieves all of these desired properties.*

To realize HiRED, our key design leverages two crucial insights from attention maps in vision encoders. The first insight is that attention maps of the class token (CLS) from initial layers are closely correlated with the visual contents and can be used to identify the main objects and irrelevant backgrounds in an image. To allocate more visual tokens to a partition with more content, we introduce the *visual content score* (which represents the amount of visual content a partition carries) as the token budget for each sub-images.

Second, we have observed that attention maps of CLS from final layers can provide insight into the tokens that carry the key image features. Therefore, we compute the CLS attention (aggregated across multiple heads) from the final layer as *feature importance score* and select visual tokens with the highest feature importance score according to the allocated budget. *By leveraging these useful insights from attention maps in vision encoders, we design a lightweight yet efficient algorithm for budget distribution and token dropping, two key components of HiRED.*

Finally, we implement and evaluate HiRED based on LLaVA-Next (Liu et al. 2024a), a popular open-source high-resolution VLM. Our experimental results show that HiRED with 20% token budget on LLaVA-Next-7B increases token generation throughput by  $4.7\times$ , reduces the response latency (time-to-first-token) by 15 seconds, and saves the GPU memory usage by 2.3 GB on an NVIDIA TESLA P40 GPU. Furthermore, HiRED achieves significantly higher accuracy than the baselines<sup>1</sup> (PruMerge and PruMerge+).

## 2 Related Work

We categorize highly related works into three groups.

**Lightweight Architecture.** Some traditional methods aim to downsize VLMs, such as LLaVA-Phi-2.7B (Zhu et al. 2024), TinyLLaVA-3.1B (Zhou et al. 2024), and MobileVLM-3B (Chu et al. 2023) but significantly sacrifice

<sup>1</sup>We chose PruMerge and PruMerge+ as our primary baselines because they utilize early-dropping mechanisms similar to ours. While TokenCorrCompressor is another early-dropping method, it is specifically designed for document understanding models and was not publicly available at the time of writing, making direct comparison infeasible. FastV and FlexAttention, though designed to reduce inference costs through sparse attention during the LLM decoding phase, still process many visual tokens in the earlier layers, resulting in inefficiency in terms of latency and memory compared to early-dropping methods.

reasoning abilities due to the reduced number of parameters. Techniques like model quantization (Dettmers et al. 2022) and weight pruning or masking (Sun et al. 2024) further reduce resource demands but do not address the critical issue of excessive visual tokens. Most of these traditional methods cannot be applied in a plug-and-play manner as they require training from scratch or fine-tuning to construct a new lightweight model or decide which neurons to prune.

**Sparse Attention Computation in LLM.** These methods aim to skip attention computation for less important visual tokens (i.e., tokens with lower attention scores) during the LLM decoding phase. FastV (Chen et al. 2024) identifies important visual tokens in the initial layers of the LLM and skips them in subsequent layers, but it is not designed for high-resolution VLMs. While FlexAttention (Li et al. 2024a) can handle high-resolution images, it does not allow control over the number of visual tokens based on resource constraints. More importantly, since these methods drop tokens during the LLM decoding phase, they still require processing excessive visual tokens in the initial layers (whereas we drop tokens before the LLM stage), thus failing to achieve substantial improvements in inference speed or memory reduction.

**Early Dropping of Visual Tokens.** These methods drop visual tokens from the image encoding stage before feeding them to LLM backbone for greater efficiency. TokenCorrCompressor (Zhang et al. 2024c) identifies repetitive whitespace patterns in document images through token-to-token cosine similarity and drops them. However, it is focused on the document understanding task only. PruMerge (Shang et al. 2024) prunes out visual tokens with low `CLS` attention and merges them with selected tokens. An upgraded version, PruMerge+, selects additional spatial tokens to mitigate information loss. Since PruMerge is designed for low-resolution VLMs, the model accuracy degrades significantly for high-resolution VLMs (see Section 5.1). Moreover, these methods lack control over the number of visual tokens within the memory budget, which is essential in resource-constrained environments.

### 3 Key Insights

**Sparse visual tokens with high attention scores.** The LLM backbone processes visual, text, and system tokens together in a typical VLM. To understand the nature of visual tokens, we investigate the attention scores of all tokens in the LLM decoding phase in Fig. 2a.

We randomly select samples from TextVQA (Singh et al. 2019), ScienceQA (Lu et al. 2022), and DocVQA (Mathew, Karatzas, and Jawahar 2021) and perform inference using LLaVA-Next-7B. While visual tokens account for 80-90% of total tokens in LLM, Fig. 2a shows that they receive significantly less attention than other token types. To further examine the gap between tokens with high and low attention scores, we compute the Cumulative Distribution Function (CDF) of attention scores for the top visual tokens with the highest attention scores, as illustrated in Fig. 2b. The CDF clearly indicates that a small subset of visual tokens bring most of the context from the image to the LLM.

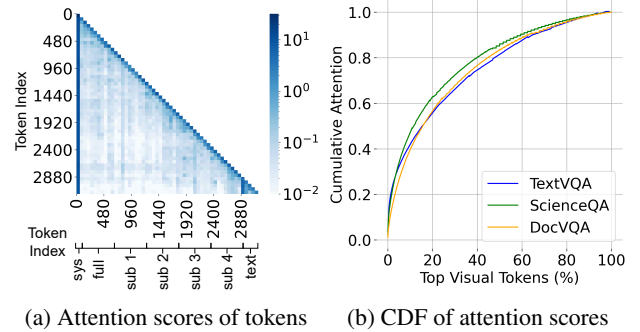


Figure 2: The sparse nature of visual tokens is evident from the attention score distribution of tokens during the LLM decoding phase. (a) demonstrates that visual tokens receive relatively less attention than system and text tokens. (b) shows that the top 20% and 40% of visual tokens receive about 60% and 80% of total attention, respectively, in randomly picked samples across benchmarks.

Table 2: Counting the origin of the top 10% and 20% visual tokens for the image partitions shown in Fig. 1.

	Full	Sub-1	Sub-2	Sub-3	Sub-4
10% (= 288 tokens)	37	12	29	84	126
20% (= 576 tokens)	94	40	61	148	234

**Insight 1 (Visual token sparsity)** *Despite the large number of visual tokens, only a small subset is important in the LLMs generation phase, suggesting an opportunity to drop less important tokens without sacrificing accuracy.*

**Various Importance of Sub-images.** Previously (in section 1), we discuss how *dynamic partitioning* can significantly boost model accuracy by encoding global and detailed local representation through full and sub-image partitions. To gain further insights into the contribution of image partitions in the LLM decoding phase, we count the number of tokens with the highest attention for each image partition as shown in Table 2. It demonstrates that the distribution of top visual tokens varies across different image partitions.

**Insight 2 (Sub-images with different content amounts)** *The variation in the visual content weights of image partitions suggests that some partitions may allow more token dropping than others.*

### 4 Our Design: HiRED

Only a small subset of visual tokens is crucial during the LLMs generation phase (by Insight 1) and varying importance of different image partitions (by Insight 2) presents a clear opportunity for dropping various numbers of visual tokens from image partitions a fixed token budget. Motivated by these insights, we explore the `CLS` token attention from the vision encoder to design an *early dropping* strategy based on the importance of image partitions in Section 4.1. We then present the overall design of HiRED in Section 4.2.

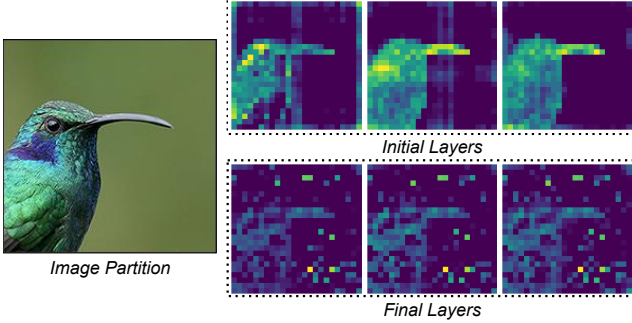


Figure 3: Attention map of ViT CLS shows distinct characteristics in the *initial layers* (0, 1, 2) and the *final layers* (21, 22, 23). The initial layers highlight the subject patches while ignoring the background, aligning mostly with the image content. The final layers, however, highlight informative patches where ViT stores most of the image features.

#### 4.1 CLS Attention-Guided Token Dropping

It is relatively straightforward to identify unimportant visual tokens (those with lower attention scores) during the LLM decoding phase, as discussed in Section 3. However, *early dropping* requires identifying important tokens before the LLM decoding phase. To achieve this, we leverage the properties of ViT, a commonly used vision encoder in VLMs (e.g., CLIP-ViT (Radford et al. 2021) in LLaVA-Next). ViTs split the image into a sequence of fixed non-overlapping patches and prepend a `CLS` token to learn features from these patches using Multihead Self-Attention (Gandelsman, Efros, and Steinhardt 2023). The attention between the `CLS` token and patch tokens indicates the relevance of each patch to the overall image features. Since these patch embeddings are later transformed into visual tokens for the LLM, guided selection of patches can effectively reduce the number of tokens. The key question remains: *How do we identify important visual tokens before the LLM phase that are crucial for generating the final response?*

To answer this, we visualize the attention map between `CLS` and patch tokens across ViT layers. Here, we have two important findings in Fig. 3: (1) Attention maps in *initial layers* reveal the main content of the input image. The highlighted patches in these attention maps correspond to visually important parts of the image. For example, in Fig. 3, the attention maps of the first three layers highlight patches derived from ‘the bird’ while ignoring background areas with no significant visual content. (2) Attention maps in *final layers* indicate the informative areas, i.e., patches that contain most of the image features. In the final layers, the highlighted patches are distributed across both the image content and the background. As the ViT processes the image, it encodes local features into corresponding patches in the initial layers. However, in the final layers, it learns the relationships between these local features and encodes them into a few background patches as global features (Darcet et al. 2023). As a result, the highlighted areas in the attention map of final layers prioritize patches that are more informative than others (Pan et al. 2021).

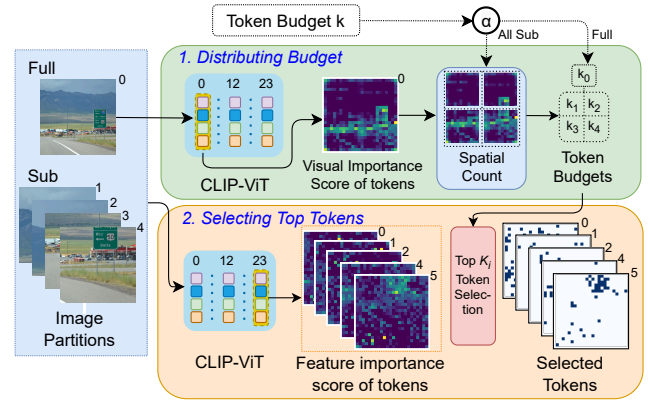


Figure 4: Design of HiRED for high-resolution VLMs to drop visual tokens before LLM. We first distribute token budgets between a full-image and sub-images and then leave selective tokens with top feature importance on each image partition within the allocated budget.

---

#### Algorithm 1: Token Dropping of HiRED

```

1: Input:  $b_{total}$ : token budget,  $\alpha$ : full-image budget ratio,  $m$ : the
   number of sub-images,  $S_{l,h}^t[p]$ : attention scores of layer  $l$  and
   head  $h$  between CLS and the  $t$ -th patch token of the  $p$ -th image
   partition, where the 0-th image partition is the full-image and others
   are sub-images,  $l_{init}$ : selected initial layer for budget distribution,
    $l_{final}$ : selected final layer for important token selection,  $T$ : total number
   of tokens in one partition

/* 1. Token Budget Distribution */
// 1-1. Calculate the token budget of the full-image
2:  $b_{full} \leftarrow \alpha \cdot b_{total}$ ;
3:  $b_{sub} \leftarrow (1 - \alpha) \cdot b_{total}$ ;
4:  $B \leftarrow token\_budget\_distribution(m, S, b_{sub}, l_{init})$ ;

/* 2. Token Dropping */
5: For  $p = 0 : m$  do
   // 2-1. Compute the feature importance scores  $I[t][p]$  for
   //  $t$ -th patch token from  $p$ -th partition
6:   For  $t = 1 : T$  do
7:      $I[t][p] \leftarrow \sum_h S_{l_{final},h}^t[p]$ ;
8:   end For
   // 2-2. Select important tokens within each budget
9:   Select  $B[p]$  tokens with the highest  $I[t][p]$ ;
10: end For

11: Function  $token\_budget\_distribution(m, S, b_{sub}, l_{init})$ 
12:   Initialize  $\bar{S}[p] \leftarrow 0$ ,  $B[p] \leftarrow 0$ ;
   // 1-2. Compute visual content scores  $\bar{S}[p]$  for  $p$ -th partition
13:   For  $p = 1 : m$  do
14:      $\bar{S}[p] \leftarrow \sum_h S_{l_{init},h}^t[p]$ ;
15:   end For
   // 1-3. Allocate the budget for each sub-image
16:    $B[p] \leftarrow b_{sub} \times \frac{\bar{S}[p]}{\sum_{p=1}^m \bar{S}[p]}$ ;
17: end Function

```

---

#### 4.2 HiRED Design

From the above two characteristics of `CLS` attention map, we design HiRED to guide the budget distribution using ini-

tial layers of ViT and the token dropping based on final layers of ViT. As outlined in Fig. 4 and Algorithm 1, HiRED consists of two phases: 1) *token budget distribution*: to distribute a given token budget across image partitions; and 2) *token dropping*: to select tokens (i.e., dropping the rest) from multiple image partitions based on their allocated budget.

**Token Budget Distribution.** Distribution of a given token budget between the image partitions is crucial to ensure the best utilization of it. To effectively distribute, we first introduce a hyperparameter  $\alpha \in [0, 1]$  to determine the token budget for the full image. The optimal value of  $\alpha$  is determined through experiments in Section 5.3. The remaining token budget is then allocated to the sub-images.

The `CLS` attention map in the initial layers aligns with the visual content of the image. The highlighted patches on the attention map indicate areas with higher visual content, suggesting that the corresponding image partitions hold greater importance. Therefore, these partitions require a higher budget allocation, i.e., a lower dropping ratio. We introduce a *visual importance* score to quantify this. We calculate this score by aggregating `CLS` attention of an initial layer (layer 0) across heads. We then apply the same partitioning (i.e., which was previously applied on the input image by *dynamic partitioning*) on the attention map. Subsequently, based on the number of highlighted patches in each partition, we calculate their *visual content scores*. In the final step, we distribute the remaining token budget to the sub-image partitions according to their scores.

**Token Dropping.** Our token-dropping strategy aims to retain tokens that carry most of the image features. We introduce a token scoring called *feature importance* to prioritize these tokens in our selection.

In Section 4.1, we observed that the final ViT layer’s `CLS` attention map highlights the informative patches coming from both the subject and background areas of an image partition. Furthermore, different heads of ViT learn different sets of features (Gandelsman, Efros, and Steinhardt 2023). We calculate the feature importance by aggregating the `CLS` attention across heads in one of the final layers (layer 22). We further experiment with the end-to-end accuracy for different choices of layers and head aggregation strategies in Section 5.3. Finally, we select tokens with the highest *feature importance* scores and drop the rest within their partition budgets. These selected tokens from all image partitions are then concatenated to form the final set of visual tokens.

## 5 Evaluation

We implemented HiRED and other baselines on LLaVA-Next using the Huggingface Transformers framework (Wolf et al. 2019). For performance evaluation, we use an entry-level accelerator, NVIDIA TESLA P40 (24 GB), with a batch size of 1.

**Downstream Tasks and Benchmarks.** We used eight benchmarks from *lmms-eval* evaluation framework (Zhang et al. 2024b) across three different task types: 1) *Visual Question Answering (Visual QA)* includes high-level object recognition benchmarks such as VQA-v2 (Goyal et al. 2017)

and ScienceQA (Lu et al. 2022); 2) *Transcription* focuses on fine-grained transcription tasks, including TextVQA (Singh et al. 2019), DocVQA (Mathew, Karatzas, and Jawahar 2021), and OCRBench (Liu et al. 2023); and 3) *Others* consists of MME (Yin et al. 2023) for perception and cognition abilities, POPE (Li et al. 2023b) for hallucination detection, and ChartQA (Masry et al. 2022) for spatial understanding.

**Baselines.** We mainly compare HiRED against two early-dropping VLM baselines similar to our approach: 1) *PruMerge*: designed for single image partitions without dynamic partitioning. For a fair comparison, we integrate our budget distribution method and apply *PruMerge*’s token-dropping algorithm separately to each image partition; and 2) *PruMerge+*: an enhanced version of *PruMerge* that additionally selects spatial tokens. It is important to note that both *PruMerge* and *PruMerge+* automatically determine the token-dropping ratio, which cannot be controlled according to resource budgets. Additionally, we include spatial pooling, a simple token-dropping strategy that uniformly samples tokens across the image. Also, LLaVA-Next using all tokens (Full) serves as the upper bound.

**Metrics.** Regarding accuracy, different downstream tasks have different performance metrics, and we use their default metrics. To measure the inference costs, we used 1) the number of visual tokens; 2) token generation throughput; 3) GPU memory usage; and 4) time to the first token (TTFT).

### 5.1 End-to-End Accuracy

We first evaluate the accuracy of LLaVA-Next (7B and 13B) with HiRED and the baseline methods across various tasks in Table 3. We also included the reported accuracy of notable models as a reference, including the closed-source models of GPT-4V and Gemini-Pro and the open-source models of Qwen-VL (7B), SPHINX (13B), Monkey (9.8B), and LLaVA-1.5 (7B and 13B).

**Accuracy vs. Token Reduction.** Evaluation results show that with a 20% token budget (i.e., a maximum of 576 tokens), HiRED achieves nearly the same accuracy as full execution (i.e., a maximum of 2880 tokens) for visual question-answering tasks. With a 40% token budget (i.e., a maximum of 1152 tokens), it maintains comparable accuracy for fine-grained transcription tasks. Interestingly, for ScienceQA and POPE, we observe an increase in accuracy with fewer tokens. This suggests that, in some cases, reducing the number of tokens improves accuracy.

**Comparison to Baselines.** We observe a greater accuracy degradation across all task categories for both *PruMerge* and *PruMerge+* methods. While these methods can dynamically adjust the token budget to retain more visual information when necessary, they still fall short compared to HiRED, particularly in transcription tasks. On average, *PruMerge* and *PruMerge+* use 10% and 55% of tokens, respectively, for transcription tasks (see section 5.2). However, even with *PruMerge+* using 55% of tokens on average, it achieves 11% to 26% lower accuracy than HiRED (20%) for TextVQA and DocVQA, respectively. Similarly, for *PruMerge* (on average 10% tokens), the accuracy is 13% to 37% lower.

Table 3: Accuracy comparison between HiRED and other baselines. In all metrics, higher values indicate better performance.  $VQA^{v2}$ , SQA, and  $VQA^T$  denotes VQA-v2, ScienceQA, and TextVQA.

Model	Budget	Visual QA		Transcription			Others		
		$VQA^{v2}$	SQA	$VQA^T$	DocVQA	OCRbench	MME	POPE	ChartQA
GPT-4V	—	—	—	78.0	88.4	645	1926	—	78.5
Gemini-Pro	—	—	—	73.5	86.5	659	—	—	81.3
Qwen-VL-Chat-7B	78.2	68.2	61.5	62.6	506	1487	—	—	66.3
SPHINX-13B	80.2	69.1	58.8	35.8	—	1560	90.8	22.5	
Monkey-9.8B	80.3	69.4	67.6	66.5	514	1505	—	—	65.1
LLaVA-1.5-7B	76.6	69.5	46.1	28.1	297	1507	85.9	18.2	
LLaVA-1.5-13B	78.3	72.9	48.7	30.3	331	1522	85.9	18.2	
LLaVA-Next-7B	Full	80.3	73.2	64.8	73.4	501	1519	87.6	54.8
Spatial	40%	77.7	68.0	57.0	58.9	369	1401	87.2	39.0
PruMerge	Auto	75.6	66.8	53.5	37.8	336	1393	85.0	28.8
PruMerge+	Auto	78.0	68.2	54.4	44.6	365	1474	87.9	30.2
HiRED	20%	77.5	73.4	61.4	60.8	475	1483	87.0	42.0
HiRED	40%	78.8	73.8	63.6	68.7	488	1474	88.2	46.5
LLaVA-Next-13B	Full	80.9	73.6	66.9	77.5	508	1572	87.1	66.2
Spatial	40%	79.1	73.0	58.8	61.3	390	1529	87.2	42.6
PruMerge	Auto	74.1	69.2	54.4	45.9	381	1471	84.9	31.0
PruMerge+	Auto	79.1	70.7	55.9	45.9	381	1480	87.5	31.0
HiRED	20%	77.9	71.9	63.6	64.3	462	1545	86.7	48.9
HiRED	40%	79.3	73.2	65.2	72.5	491	1570	87.7	53.7

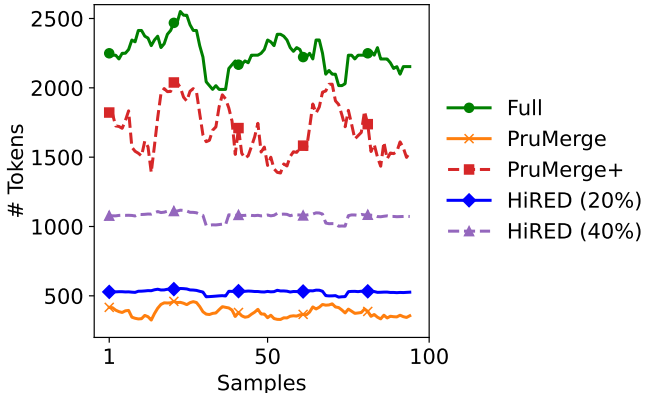


Figure 5: Number of visual tokens generated in 100 TextVQA samples for Full execution, PruMerge, PruMerge+, and HiRED with the token budget of 20% and 40%.

## 5.2 Inference Efficiency

To evaluate the inference efficiency of HiRED under various token budgets, we measure its throughput, time to first token (TTFT), and GPU memory usage. The results are presented in Table 4. We also compare the number of tokens generated by HiRED with the adaptive number of tokens generated by PruMerge and PruMerge+ in Fig. 5.

**Inference Efficiency of HiRED.** The evaluation results presented in Table 4 demonstrate the effectiveness of HiRED in achieving inference efficiency. Notably, with a 20% token

Table 4: Inference costs of the number of tokens, throughputs, TTFT, and GPU memory usage using LLaVA-Next-7B with HiRED with respect to different token budgets.

Budget	# Tokens	Throughput (tokens/sec)	TTFT (sec)	Memory (GB)
Full	2880	0.49	19.49	16.04
40%	1152	1.40	6.91	14.33
30%	864	1.83	5.30	14.04
20%	576	2.30	4.21	13.76
10%	288	3.08	3.14	13.48

budget, our method increases throughput by  $4.7\times$  compared to full execution. The time to first token is reduced by 15 seconds, which is particularly valuable for applications where low latency is crucial. Additionally, using a 20% token budget saves 2.3 GB of GPU memory due to reduced KV cache size. This reduction in memory usage may enable the use of larger batch sizes that the GPU can accommodate.

**Efficiency under Token Budget.** As shown in Fig. 5, HiRED maintains a consistent number of visual tokens for LLaVA-Next-7B under a fixed token budget (e.g., 20%). In contrast, the full model execution, PruMerge and PruMerge+ exhibit significant variation in the number of visual tokens across different samples in TextVQA. The variation in full execution arises from different partitioning based on the image aspect ratio and the removal of some padding tokens. For PruMerge and PruMerge+, the variation is due to their adap-

Table 5: Ablation study of ViT layer selection and head aggregation strategy in HiRED’s token dropping algorithm.

Choice	SQA	VQA <sup>v2</sup>	VQA <sup>T</sup>	DocVQA
ViT Layer				
Initial (0)	65.2	68.6	37.3	54.0
Middle (11)	68.0	76.1	51.9	52.0
Final (22)	<b>68.4</b>	<b>77.7</b>	<b>54.8</b>	<b>59.2</b>
Head Aggregation				
w/o	67.2	76.6	50.5	52.4
Addition	<b>68.4</b>	<b>77.7</b>	<b>54.8</b>	<b>59.2</b>

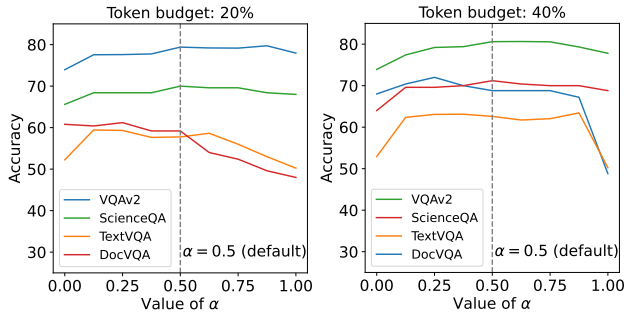


Figure 6: Choice of full-image budget ratio  $\alpha$ .

tive nature, which selects more tokens when images contain more visual information. This variation in the number of visual tokens directly impacts computational cost. Therefore, HiRED proves to be highly effective under strict resource constraints during the deployment phase.

### 5.3 Ablation Study

We evaluate the key components of HiRED and the effectiveness of our design choices through an ablation study. For this study, we select two visual question answering tasks (i.e., ScienceQA, VQAv2) and two fine-grained transcription tasks (i.e., TextVQA, DocVQA).

**Token Selection.** To understand the effectiveness of our Token Selection algorithm design, we evaluate it with different layer selection and head aggregation techniques in Table 5. Then, we apply our selection algorithm to the LLaVA-1.5-7B model. This model does not apply partitioning on the input image; hence, there is one image partition to encode. As a result, the budget distribution component is not required here. We evaluated our token dropping performance by comparing it with PruMerge and Prumerge+ for different token budgets (i.e., 20% and 40%). The results are presented in Table 6. Results show that our method with a 20% budget achieves similar or better results than PruMerge and PruMerge+, especially for text-rich tasks such as TextVQA.

**Budget Distribution.** HiRED’s budget distribution adapts to the varying importance of image partitions for efficient token use. We set the default hyperparameter  $\alpha = 0.5$  to allocate the token budget between the full image and sub-images. As shown in Fig. 6, varying  $\alpha$  impacts accuracy,

Table 6: The number of tokens and accuracy across various token selection methods using low-resolution (i.e., single partition) LLaVA-1.5-7B model.

LLaVA-1.5-7B	SQA	VQA <sup>v2</sup>	VQA <sup>T</sup>	DocVQA
Full	69.5	76.6	46.1	28.1
PruMerge	65.6	65.2	35.4	18.2
PruMerge+	66.4	75.8	36.0	20.4
HiRED (20%)	66.4	74.7	44.2	24.6
HiRED (40%)	67.2	79.0	47.0	29.4

Table 7: Accuracy of different budget distribution.

Distribution	SQA	VQA <sup>v2</sup>	VQA <sup>T</sup>	DocVQA
Equal	67.6	73.3	52.2	48.8
HiRED	<b>68.4</b>	<b>77.7</b>	<b>54.8</b>	<b>50.1</b>

with balanced distribution (e.g.,  $\alpha = 0.5$ ) yielding better results. Specifically,  $\alpha = 0$  assigns no budget to the full image, while  $\alpha = 1$  allocates the maximum. The remaining budget is distributed among sub-images based on importance. The experiment demonstrates that balancing the budget across full and sub-images is crucial, and  $\alpha = 0.5$  generally offers better results, making it our default choice.

To evaluate the significance of budget distribution in VLMs with dynamic image partitioning, we compare HiRED to a setting with equal budget distribution across image partitions. The results, shown in Table 7, illustrate that under a 10% token budget setting, HiRED’s adaptive distribution achieves higher accuracy than equal division. Distributing the budget without our method involves simply dividing it equally among partitions.

## 6 Conclusion

High-resolution VLMs can enhance accuracy for a wide range of multimodal tasks by preserving detailed image information. However, due to the excessively generated visual tokens, it is challenging to achieve efficient high-resolution VLM inference in resource-constrained environments. In this paper, we addressed this key challenge by strategically dropping visual tokens within a given token budget. Specifically, we proposed HiRED, a plug-and-play early-token-dropping framework that effectively distributes a fixed token budget among image partitions, selects the most important visual tokens accordingly, and then drops the rest of the visual tokens before the LLM decoding phase. Our evaluation results demonstrated that HiRED substantially improves inference throughput, reduces time-to-first-token latency, and saves GPU memory usage while maintaining superior accuracy of high-resolution VLMs across diverse multimodal tasks. We hope that HiRED will shed light on future research into optimizing VLMs for more efficient and scalable performance in resource-constrained environments.

## References

Achiam, J.; Adler, S.; Agarwal, S.; Ahmad, L.; Akkaya, I.; Aleman, F. L.; Almeida, D.; Altenschmidt, J.; Altman, S.; Anadkat, S.; et al. 2023. Gpt-4 Technical Report. *arXiv preprint arXiv:2303.08774*.

Bai, J.; Bai, S.; Yang, S.; Wang, S.; Tan, S.; Wang, P.; Lin, J.; Zhou, C.; and Zhou, J. 2023. Qwen-vl: A versatile vision-language model for understanding, localization, text reading, and beyond.

Cai, M.; Yang, J.; Gao, J.; and Lee, Y. J. 2024. Matryoshka Multimodal Models. *arXiv preprint arXiv:2405.17430*.

Chen, L.; Zhao, H.; Liu, T.; Bai, S.; Lin, J.; Zhou, C.; and Chang, B. 2024. An Image is Worth 1/2 Tokens After Layer 2: Plug-and-Play Inference Acceleration for Large Vision-Language Models. *arXiv:2403.06764*.

Chen, Z.; Pekis, A.; and Brown, K. 2024. Advancing High Resolution Vision-Language Models in Biomedicine. *arXiv preprint arXiv:2406.09454*.

Chu, X.; Qiao, L.; Lin, X.; Xu, S.; Yang, Y.; Hu, Y.; Wei, F.; Zhang, X.; Zhang, B.; Wei, X.; et al. 2023. Mobilevlm: A fast, reproducible and strong vision language assistant for mobile devices. *arXiv preprint arXiv:2312.16886*.

Darcet, T.; Oquab, M.; Mairal, J.; and Bojanowski, P. 2023. Vision transformers need registers. *arXiv preprint arXiv:2309.16588*.

Dettmers, T.; Lewis, M.; Belkada, Y.; and Zettlemoyer, L. 2022. Gpt3. int8 () 8-bit matrix multiplication for transformers at scale. *Advances in Neural Information Processing Systems*, 35: 30318–30332.

Dong, X.; Zhang, P.; Zang, Y.; Cao, Y.; Wang, B.; Ouyang, L.; Zhang, S.; Duan, H.; Zhang, W.; Li, Y.; et al. 2024. Internlm-xcomposer2-4khd: A pioneering large vision-language model handling resolutions from 336 pixels to 4k hd. *arXiv preprint arXiv:2404.06512*.

Gandelsman, Y.; Efros, A. A.; and Steinhardt, J. 2023. Interpreting CLIP’s Image Representation via Text-Based Decomposition. *arXiv preprint arXiv:2310.05916*.

Goyal, Y.; Khot, T.; Summers-Stay, D.; Batra, D.; and Parikh, D. 2017. Making the v in vqa matter: Elevating the role of image understanding in visual question answering. In *Proceedings of the IEEE conference on computer vision and pattern recognition*, 6904–6913.

Hu, A.; Xu, H.; Ye, J.; Yan, M.; Zhang, L.; Zhang, B.; Li, C.; Zhang, J.; Jin, Q.; Huang, F.; et al. 2024. mplug-docowl 1.5: Unified structure learning for ocr-free document understanding. *arXiv preprint arXiv:2403.12895*.

Li, J.; Chen, D.; Cai, T.; Chen, P.; Hong, Y.; Chen, Z.; Shen, Y.; and Gan, C. 2024a. FlexAttention for Efficient High-Resolution Vision-Language Models. *arXiv preprint arXiv:2407.20228*.

Li, L.; Yin, Y.; Li, S.; Chen, L.; Wang, P.; Ren, S.; Li, M.; Yang, Y.; Xu, J.; Sun, X.; et al. 2023a. M<sup>3</sup> IT: A Large-Scale Dataset towards Multi-Modal Multilingual Instruction Tuning. *arXiv preprint arXiv:2306.04387*.

Li, Y.; Du, Y.; Zhou, K.; Wang, J.; Zhao, W. X.; and Wen, J.-R. 2023b. Evaluating object hallucination in large vision-language models. *arXiv preprint arXiv:2305.10355*.

Li, Z.; Yang, B.; Liu, Q.; Ma, Z.; Zhang, S.; Yang, J.; Sun, Y.; Liu, Y.; and Bai, X. 2024b. Monkey: Image resolution and text label are important things for large multi-modal models. In *Proceedings of the IEEE/CVF Conference on Computer Vision and Pattern Recognition*, 26763–26773.

Lin, Z.; Liu, C.; Zhang, R.; Gao, P.; Qiu, L.; Xiao, H.; Qiu, H.; Lin, C.; Shao, W.; Chen, K.; et al. 2023. SPHINX: The joint mixing of weights, tasks, and visual embeddings for multi-modal large language models. *arXiv preprint arXiv:2311.07575*.

Liu, H.; Li, C.; Li, Y.; Li, B.; Zhang, Y.; Shen, S.; and Lee, Y. J. 2024a. Llava-next: Improved reasoning, OCR, and World Knowledge.

Liu, Y.; Li, Z.; Yang, B.; Li, C.; Yin, X.; Liu, C.-l.; Jin, L.; and Bai, X. 2023. On the hidden mystery of ocr in large multimodal models. *arXiv preprint arXiv:2305.07895*.

Liu, Y.; Yang, B.; Liu, Q.; Li, Z.; Ma, Z.; Zhang, S.; and Bai, X. 2024b. Textmonkey: An ocr-free large multi-modal model for understanding document. *arXiv preprint arXiv:2403.04473*.

Lu, P.; Mishra, S.; Xia, T.; Qiu, L.; Chang, K.-W.; Zhu, S.-C.; Tafjord, O.; Clark, P.; and Kalyan, A. 2022. Learn to explain: Multimodal reasoning via thought chains for science question answering. *Advances in Neural Information Processing Systems*, 35: 2507–2521.

Masry, A.; Long, D. X.; Tan, J. Q.; Joty, S.; and Hoque, E. 2022. Chartqa: A benchmark for question answering about charts with visual and logical reasoning. *arXiv preprint arXiv:2203.10244*.

Mathew, M.; Karatzas, D.; and Jawahar, C. 2021. Docvqa: A dataset for vqa on document images. In *Proceedings of the IEEE/CVF winter conference on applications of computer vision*, 2200–2209.

McKinzie, B.; Gan, Z.; Fauconnier, J.-P.; Dodge, S.; Zhang, B.; Dufter, P.; Shah, D.; Du, X.; Peng, F.; Weers, F.; et al. 2024. Mm1: Methods, analysis & insights from multimodal llm pre-training. *arXiv preprint arXiv:2403.09611*.

Pan, B.; Panda, R.; Jiang, Y.; Wang, Z.; Feris, R.; and Oliva, A. 2021. IA-RED<sup>2</sup>: Interpretability-Aware Redundancy Reduction for Vision Transformers. *Advances in Neural Information Processing Systems*, 34: 24898–24911.

Radford, A.; Kim, J. W.; Hallacy, C.; Ramesh, A.; Goh, G.; Agarwal, S.; Sastry, G.; Askell, A.; Mishkin, P.; Clark, J.; et al. 2021. Learning transferable visual models from natural language supervision. In *International conference on machine learning*, 8748–8763. PMLR.

Reid, M.; Savinov, N.; Teplyashin, D.; Lepikhin, D.; Lilliacrap, T.; Alayrac, J.-b.; Soricut, R.; Lazaridou, A.; Firat, O.; Schrittwieser, J.; et al. 2024. Gemini 1.5: Unlocking multimodal understanding across millions of tokens of context. *arXiv preprint arXiv:2403.05530*.

Shang, Y.; Cai, M.; Xu, B.; Lee, Y. J.; and Yan, Y. 2024. LLaVA-PruMerge: Adaptive Token Reduction for Efficient Large Multimodal Models. *arXiv:2403.15388*.

Singh, A.; Natarajan, V.; Shah, M.; Jiang, Y.; Chen, X.; Batra, D.; Parikh, D.; and Rohrbach, M. 2019. Towards VQA Models That Can Read. In *Proceedings of the IEEE/CVF Conference on Computer Vision and Pattern Recognition (CVPR)*.

Sun, M.; Liu, Z.; Bair, A.; and Kolter, J. Z. 2024. A Simple and Effective Pruning Approach for Large Language Models. In *The Twelfth International Conference on Learning Representations*.

Wolf, T.; Debut, L.; Sanh, V.; Chaumond, J.; Delangue, C.; Moi, A.; Cistac, P.; Rault, T.; Louf, R.; Funtowicz, M.; et al. 2019. Huggingface’s transformers: State-of-the-art natural language processing. *arXiv preprint arXiv:1910.03771*.

Yin, S.; Fu, C.; Zhao, S.; Li, K.; Sun, X.; Xu, T.; and Chen, E. 2023. A survey on multimodal large language models. *arXiv preprint arXiv:2306.13549*.

Zhang, D.; Yu, Y.; Li, C.; Dong, J.; Su, D.; Chu, C.; and Yu, D. 2024a. Mm-llms: Recent advances in multimodal large language models. *arXiv preprint arXiv:2401.13601*.

Zhang, K.; Li, B.; Zhang, P.; Pu, F.; Cahyono, J. A.; Hu, K.; Liu, S.; Zhang, Y.; Yang, J.; Li, C.; et al. 2024b. LMMs-Eval: Reality Check on the Evaluation of Large Multimodal Models. *arXiv preprint arXiv:2407.12772*.

Zhang, R.; Lyu, Y.; Shao, R.; Chen, G.; Guan, W.; and Nie, L. 2024c. Token-level Correlation-guided Compression for Efficient Multimodal Document Understanding. *arXiv preprint arXiv:2407.14439*.

Zhou, B.; Hu, Y.; Weng, X.; Jia, J.; Luo, J.; Liu, X.; Wu, J.; and Huang, L. 2024. Tinyllava: A framework of small-scale large multimodal models. *arXiv preprint arXiv:2402.14289*.

Zhu, Y.; Zhu, M.; Liu, N.; Ou, Z.; Mou, X.; and Tang, J. 2024. LLaVA- $\phi$ : Efficient Multi-Modal Assistant with Small Language Model. *arXiv preprint arXiv:2401.02330*.